# Partial restoration of brain dystrophin by tricyclo-DNA antisense oligonucleotides alleviates emotional deficits in mdx52 mice

Amel Saoudi, Sacha Barberat, Olivier Le Coz, Ophélie Vacca, Mathilde Doisy Caquant, Thomas Tensorer, Eric Sliwinski, Luis Garcia, Francesco M. Muntoni, Cyrille Vaillend, et al.

▶ **To cite this version:**

Amel Saoudi, Sacha Barberat, Olivier Le Coz, Ophélie Vacca, Mathilde Doisy Caquant, et al.. Partial restoration of brain dystrophin by tricyclo-DNA antisense oligonucleotides alleviates emotional deficits in mdx52 mice. Molecular Therapy - Nucleic Acids, 2023, 32, pp.173-188. 10.1016/j.omtn.2023.03.009 . hal-04106304

**HAL Id: hal-04106304**
**https://hal.science/hal-04106304**

Submitted on 30 Jun 2023

**HAL** is a multi-disciplinary open access archive for the deposit and dissemination of scientific research documents, whether they are published or not. The documents may come from teaching and research institutions in France or abroad, or from public or private research centers.

L'archive ouverte pluridisciplinaire **HAL**, est destinée au dépôt et à la diffusion de documents scientifiques de niveau recherche, publiés ou non, émanant des établissements d'enseignement et de recherche français ou étrangers, des laboratoires publics ou privés.

Distributed under a Creative Commons Attribution 4.0 International License

Molecular Therapy
Nucleic Acids
Original Article

# Partial restoration of brain dystrophin by tricyclo-DNA antisense oligonucleotides alleviates emotional deficits in *mdx52* mice

Amel Saoudi,[1,2] Sacha Barberat,[1] Olivier le Coz,[1] Ophélie Vacca,[1] Mathilde Doisy Caquant,[1] Thomas Tensorer,[3] Eric Sliwinski,[3] Luis Garcia,[1] Francesco Muntoni,[4] Cyrille Vaillend,[2,5] and Aurélie Goyenvalle[1,5]

[1]Université Paris-Saclay, UVSQ, Inserm, END-ICAP, 78000 Versailles, France; [2]Université Paris-Saclay, CNRS, Institut des Neurosciences Paris-Saclay, 91400 Saclay, France; [3]SQY Therapeutics – Synthena, UVSQ, 78180 Montigny le Bretonneux, France; [4]The Dubowitz Neuromuscular Centre, Developmental Neurosciences Research and Teaching Department, Great Ormond Street Institute of Child Health, University College London, WC1N 1EH London, UK

**The *mdx52* mouse model recapitulates a frequent mutation profile associated with brain involvement in Duchenne muscular dystrophy. Deletion of exon 52 impedes expression of two dystrophins (Dp427, Dp140) expressed in brain, and is eligible for therapeutic exon-skipping strategies. We previously showed that *mdx52* mice display enhanced anxiety and fearfulness, and impaired associative fear learning. In this study, we examined the reversibility of these phenotypes using exon 51 skipping to restore exclusively Dp427 expression in the brain of *mdx52* mice. We first show that a single intracerebroventricular administration of tricyclo-DNA antisense oligonucleotides targeting exon 51 restores 5%–15% of dystrophin protein expression in the hippocampus, cerebellum, and cortex, at stable levels between 7 and 11 week after injection. Anxiety and unconditioned fear were significantly reduced in treated *mdx52* mice and acquisition of fear conditioning appeared fully rescued, while fear memory tested 24 h later was only partially improved. Additional restoration of Dp427 in skeletal and cardiac muscles by systemic treatment did not further improve the unconditioned fear response, confirming the central origin of this phenotype. These findings indicate that some emotional and cognitive deficits associated with dystrophin deficiency may be reversible or at least improved by partial postnatal dystrophin rescue.**

## INTRODUCTION

Duchenne muscular dystrophy (DMD) is a neuromuscular disease that affects 1:5,000 male births and is associated with non-progressive cognitive, behavioral and neuropsychiatric comorbidities.[1–3] DMD is caused by mutations in the dystrophin (*DMD*) gene that encodes multiple dystrophin proteins (Dp). Dystrophins are membrane-bound proteins involved in receptor and ion channel clustering in a cell- and tissue-specific manner. The dystrophins differ by their molecular weight, expression, and function. The full-length dystrophins, Dp427 M/C/P, are expressed in muscles (Dp427M) as well as in central GABAergic synapses in brain (Dp427C) and cerebellum where they contribute to the synaptic clustering of $GABA_A$ receptors.[4,5] The smaller C-terminal brain dystrophins are expressed from independent internal promoters: Dp260 is selectively expressed in the retina, Dp140 shows enriched expression in the fetal human brain but its cellular localization in adult brain is still unclear,[5,6] and Dp71 is expressed in excitatory synapses as well as in astrocyte endfeet forming the blood-brain barrier (BBB), where it plays a role in aquaporin 4 (AQP4) regulation.[7] Mutations in the *DMD* gene lead to muscular dystrophy due to the loss of the muscle dystrophin, while the nature and severity of brain alterations in DMD patients depend on the position of the mutation and on the type and number of dystrophins affected by the mutation.[3] While proximal mutations inducing the loss of the full-length Dp427 are generally associated with very modest effect on cognitive function, the more distal ones are associated with more severe deficits due to the cumulative loss of several brain dystrophins.[8,9] Functional studies of different DMD mouse models provided an essential contribution to our understanding of the affected brain mechanisms depending on the position of the mutation and loss of different dystrophins.[10–12] We previously demonstrated that the exon52-deleted *mdx52* mouse model,[13] lacking Dp427, Dp260, and Dp140, shows stronger emotional alterations compared with the original Dp427-deficient-*mdx* mouse model.[10] Indeed, the mutation is located in a "hot spot" region frequently found to be mutated in DMD patients (65%).[1,3,9] The development of therapeutic approaches in this mouse model is thus of great interest, as it directly translates to patients' condition. One of the most promising therapeutic strategies for DMD aims to restore the open reading frame to express an internally deleted but still functional protein. This so-called exon-skipping strategy is based on the use of antisense oligonucleotides (ASOs) that interfere with splicing signals or

Received 20 October 2022; accepted 16 March 2023;
https://doi.org/10.1016/j.omtn.2023.03.009.

[5]These authors contributed equally

**Correspondence:** Cyrille Vaillend, Université Paris-Saclay, CNRS, Institut des Neurosciences Paris-Saclay, 91400 Saclay, France.
**E-mail:** cyrille.vaillend@universite-paris-saclay.fr
**Correspondence:** Aurélie Goyenvalle, Université Paris-Saclay, UVSQ, Inserm, END-ICAP, 78000 Versailles, France.
**E-mail:** aurelie.goyenvalle@uvsq.fr


This is an open access article under the CC BY license (http://creativecommons.org/licenses/by/4.0/).

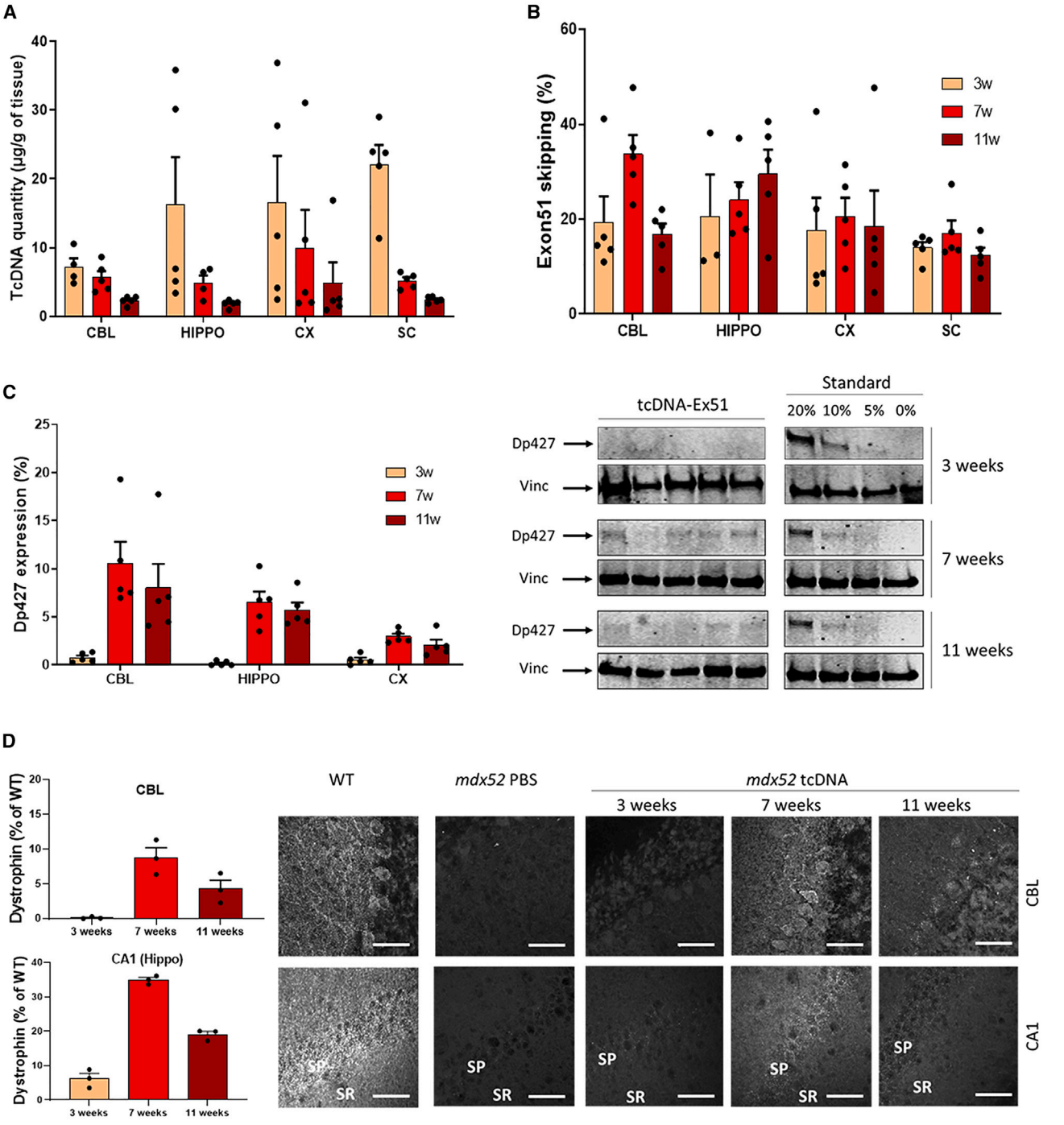


**Figure 1. Optimal time frame following i.c.v. delivery of tcDNA-Ex51**

(A) Quantification of fluorescent hybridization of tcDNA-Ex51 in various CNS tissues (CBL, cerebellum; HIPPO, hippocampus; CX, cortex; SC, the cervical part of the spinal cord) at 3, 7, and 11 weeks after i.c.v. administration. Results are expressed as mean ± SEM; n = 5 mice per group. (B) Quantification of exon 51-skipping levels by qRT-PCR in same tissues as above at 3, 7, and 11 weeks after i.c.v. administration. (C) Dp427 protein restoration by western blot in the same brain regions as above, at 3, 7, and 11 weeks after i.c.v. administration (mean ± SEM; n = 5 mice per group). Immunoblots shown in the right panel are representative examples of dystrophin restoration in the hippocampus at the different time points. A four-point standard curve made of 0%, 5%, 10%, and 20% of WT lysate (mixed with *mdx52* lysate) was loaded for

*(legend continued on next page)*

regulatory elements in the exon or intron, thus leading to the skipping of the targeted exon at the precursor (pre-)mRNA level.[14–16] Previous studies in *mdx52* mice demonstrated the therapeutic potential of the exon-skipping approach to restore expression of Dp427 in muscles using naked ASO[17] or vectorized sequences in AAV-U7snRNA vector.[18] The feasibility of antisense-based therapies has been demonstrated in clinical trials and several ASO drugs have now been conditionally approved by the FDA.[19] However, none of the currently approved ASO drugs are capable of addressing DMD brain comorbidities, mostly because of their inability to cross the BBB. Yet novel ASO chemistries or conjugates are currently being developed and may offer promising tools to treat both the dystrophic phenotype and the central deficits associated with the lack of brain dystrophin. Among these, we have previously demonstrated that tricyclo-DNA (tcDNA)-based ASOs display unprecedented uptake in many tissues including cardiac muscle and central nervous system (CNS) after intravenous administration in mouse models of DMD[20–22] and SMA.[23] More recently, we have shown that local administration of tcDNA-based ASO in the brain of *mdx* mice lacking only Dp427 alleviates some cognitive deficits associated with DMD.[24]

In this study, we aimed to investigate the impact of postnatal restoration of brain Dp427 in the more severe *mdx52* model, which is representative of a larger subpopulation of DMD patients. For this purpose, we used a tcDNA-ASO conjugated to palmitic acid[22] and targeting dystrophin exon 51, to restore Dp427 exclusively. Given that exon 51 contains the start codon for Dp140, skipping of exon 51 indeed cannot restore Dp140 expression. We first determined the optimal therapeutic window following intracerebroventricular (i.c.v.) microinjection of tcDNA-Ex51 and then assessed its potential in rescuing behavior, using tests in which *mdx52* mice typically show deficits.[10] Anxiety, unconditioned fear, and conditioned fear learning and memory were successively assessed in treated *mdx52* mice. The efficacy of the treatment was also analyzed at the molecular level, and we further evaluated the contribution of partial Dp427 restoration by systemic injection in muscles and heart to rule out the possibility of a peripheral contribution to the behavioral improvements observed.

## RESULTS

### Optimal time frame for Dp427 restoration following i.c.v. delivery of tcDNA-Ex51

We first investigated the extent and duration of dystrophin restoration following a single injection of tcDNA-Ex51 in each lateral ventricle (bilateral i.c.v. injection) to define the optimal time frame for behavioral studies. For this experiment, 8-week-old *mdx52* mice received i.c.v. injections of a total 400 μg of tcDNA-Ex51. As described previously for tcDNA targeting exon 23,[24] the maximal dose was 400 μg, a limitation related to the solubility of the tcDNA-ASOs taken from a 40 mg/mL stock solution for bilateral injections of a 10-μL maximal volume. Distinct groups were analyzed at three different time points: 3, 7, and 11 weeks after the i.c.v. injections. For each time point, we examined different regions of the CNS: the cerebellum, hippocampus, cortex, and the cervical part of the spinal cord. We first analyzed the biodistribution of the tcDNA by quantifying the amount of tcDNA-Ex51 in each structure using a fluorescent hybridization assay. Results presented in Figure 1A indicate that tcDNA-Ex51 was homogeneously distributed (structure effect, $p = 0.2429$) in the different regions after i.c.v. administration and that the quantity was decreasing with time as expected from previous studies (time effect, $p = 0.0036$). We then estimated the efficacy of the treatment by quantifying the levels of exon 51 skipping in the different brain regions by real time TaqMan PCR quantification (Figure 1B).

The i.c.v. injection of 400 μg of tcDNA-Ex51 induced a mean of 30% of exon 51 skipping across the various structures and levels of exon skipping appeared stable between 3 and 11 weeks after the treatment (time effect, $p = 0.3071$, structure × time point effect ($F(6,34) = 1.195$, $p = 0.3327$). No exon 51 skipping was detected in skeletal muscles (data not shown), indicating no peripheral effect after i.c.v. delivery as shown previously.[24] i.c.v. injection of 400 μg of a control (sense) tcDNA induced no exon skipping in any of the analyzed regions (Figure S1). We then quantified the restoration of the dystrophin protein (Dp427) by western blot in the cerebellum, hippocampus, and cortex at the different time points (Figure 1C). Three weeks after i.c.v. administration, the levels of Dp427 were very low (~1%), while after 7 weeks we detected between 3% and 10% of Dp427 production in the different brain regions (structure effect, $p = 0.0042$). These levels were found to be stable between 7 and 11 weeks (time effect, $p = 0.6494$). Despite the presence of a substantial amount of skipped mRNAs, we could not detect any protein restoration in the cervical part of the spinal cord, which may be due to the very low levels of Dp427 normally expressed in this structure (Figure S2).

Dp427 re-expression was also confirmed in *in situ* sections by immunofluorescent staining. Dystrophin is normally expressed in inhibitory synapses of pyramidal neurons, showing typical punctate staining around their soma in the stratum pyramidal (SP) and in the proximal dendritic layer of the stratum radiatum (SR) within the CA1-CA3 hippocampal subfields. Accordingly, Figure 1D shows that dystrophin expression was indeed characterized by a punctate immunoreactive signal reflecting synaptic expression in wild-type (WT) mice as well as in tcDNA-Ex51-treated *mdx52* mice, while it was completely absent in PBS-treated *mdx52* mice. The level of dystrophin restoration was estimated using a semi-quantitative approach based on confocal image analysis in synapses of hippocampal neurons and in the Purkinje cell layer (PCL) and molecular cell layer (MCL) of the cerebellum.[4] TcDNA-Ex51-treated *mdx52* mice displayed

quantification (the same standard is shown for 7 and 11 weeks since they were loaded on the same gel). Vinculin used as control for normalization. (D) Detection of the restored dystrophin protein by immunofluorescence in the cerebellar Purkinje cell layer and the molecular cell layer, as well as the stratum pyramidale (SP) and proximal stratum radiatum (SR) of the CA1 hippocampal subfield, as indicated. Groups of WT, *mdx52* mice injected with PBS (*mdx52* PBS), and tcDNA-Ex51 (*mdx52* tcDNA) were compared at 3, 7, and 11 week after i.c.v. administration (mean ± SEM; n = 3 mice per group). Scale bars, 12 μm.

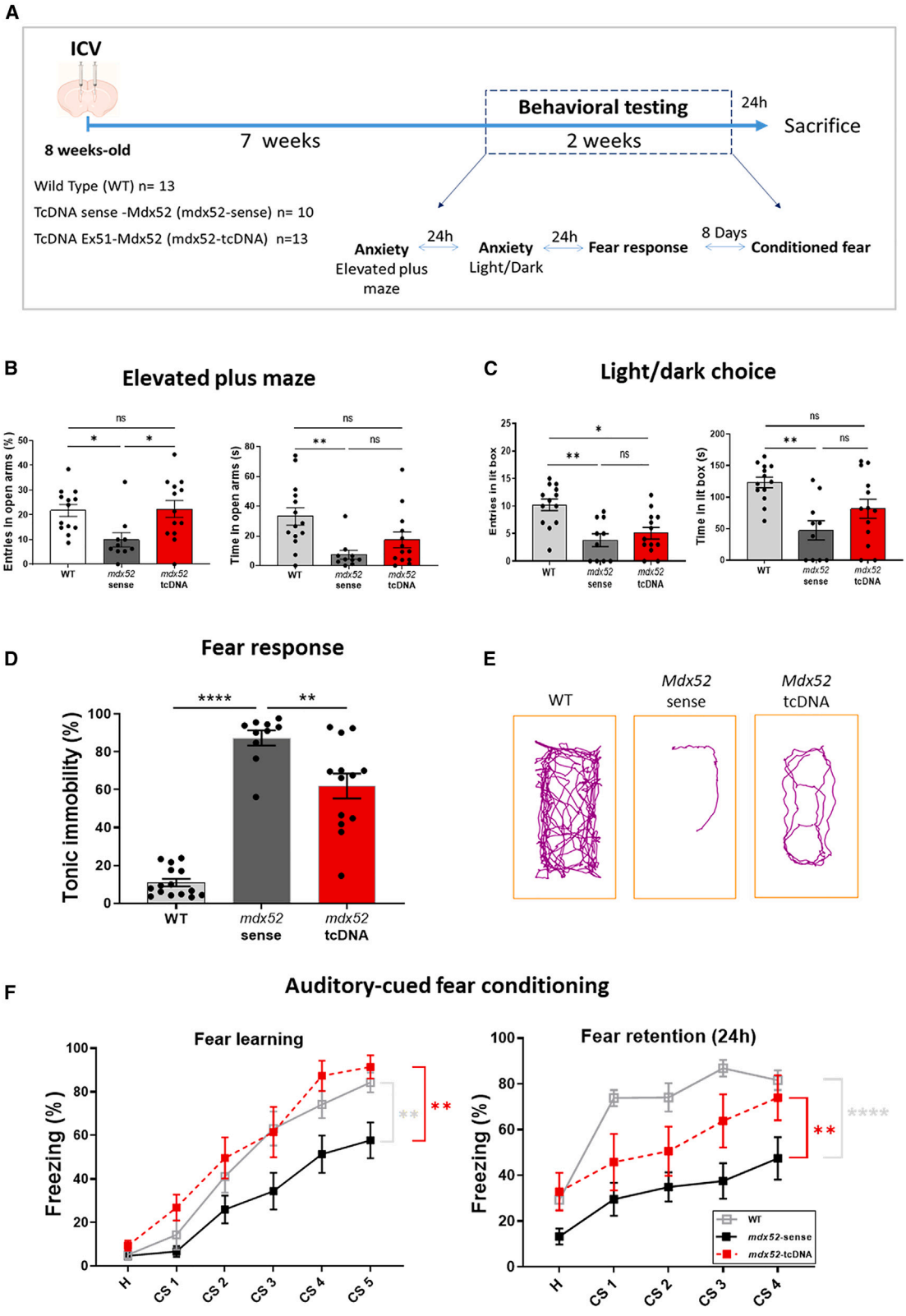


*(legend on next page)*

significant levels of dystrophin re-expression, compared with untreated *mdx52* mice, in the MCL and PCL of the cerebellum at 7- and 11-week time points, ranging from 3% to 12%, while it was barely detectable at 3 weeks. In the SP and SR layers of the CA1 region of the hippocampus, Dp427 was already detectable at low levels (∼6%) at 3 weeks, reached approximately 30% at 7 weeks, and then slightly decreased to 20% at 11 weeks (Figure 1D). Dp427 expression was also detected at low levels in the basolateral nucleus of the amygdala, although quite variably between individuals which prevented accurate quantification (Figure S3). Overall, these findings indicate that the optimal therapeutic window is between 7 and 11 weeks after i.c.v. administration, when exon 51 skipping and Dp427 restoration are at their highest levels in the different brain structures.

### Effect of partial Dp427 restoration on *mdx52* mice impaired behavior

To assess the functionality of the restored Dp427, groups of 8-week-old *mdx52* and WT littermates received i.c.v. injections as follows: n = 13 *mdx52* mice received the tcDNA-Ex51 (*mdx52*-tcDNA), n = 10 *mdx52* mice received the control sense sequence of tcDNA (*mdx52*-sense), and n = 13 WT mice received the saline solution. Within the therapeutic window determined above (between 7 and 9 weeks after the i.c.v.), the three groups of mice were submitted to behavioral testing, using a selection of tests with low motor demand that had previously highlighted robust emotional-related deficits in *mdx52* mice.[10]

The behavioral testing consisted of four consecutive tests separated by at least a 24-h interval (Figure 2A), starting with measures of anxiety in the elevated plus maze then in the light dark choice. In the elevated plus-maze test, anxiety results from the threat induced by the void in the elevated open arms. Global activity in the maze, reflected by the total number of arms visited, was comparable in treated and untreated *mdx52* groups (Figure S4A), while an increased number of entries into open arms was only observed in *mdx52*-tcDNA (Figure S4B). This indicates that the increased number of entries into open arms in the *mdx52*-tcDNA group could not be directly attributed to a change in global activity. As shown in Figure 2B the percent of entries in the open arms was significantly reduced in the control *mdx52-sense* group compared with WT ($p = 0.0242$), a behavioral deficit that is consistent with the deficits previously characterized in this model. In contrast, in the tcDNA-Ex51-treated *mdx52* group the percent of entries was comparable with the WT group ($p > 0.9999$). The time spent in open arms also appeared similar between the WT and tcDNA-Ex51 groups ($p = 0.1527$) (Figure 2B), which further supports that this phenotype was rescued in this test.

The light/dark choice test that we described previously[10] is based on the choice given to the mice to stay in a secure dark compartment or to explore an anxiogenic (brightly lit) compartment characterized by a gradient of illumination from the trap door (50 Lx) to the end of the compartment (600 Lx). The number of entries into the lit box was found to be comparable between the WT group and the control group *mdx52*-sense, as shown in Figure 2C. However, for the time spent in the lit compartment, which is a good marker of the anxiety level in this test, control *mdx52* mice spent significantly less time in the lit box compared with WT mice ($p = 0.0027$), thus confirming their anxiety-related phenotype. In contrast, tcDNA-Ex51-treated *mdx52* mice spent as much time as the WT mice (ns, $p = 0.1786$) (Figure 2C). The results of these two tests of anxiety suggest that tcDNA-Ex51 treatment has the potential to partly rescue the anxiety phenotype of *mdx52* mice.

The third test/manipulation evaluated the stress-induced freezing response, which is typically characterized by a complete tonic immobilization of the mouse, except for respiration, in mouse models of DMD. It is expressed as the percent time spent in tonic immobility (percent freezing) during a 5-min period following a brief (15 s) manual scruff-restraint, which is considered as a measure of unconditioned fear. Manual restraint did not induce a fear response in the WT mice (mean percent time spent immobile <20%) (Figure 2D). In contrast, in control sense-treated *mdx52* mice, the fear response was clearly expressed (>85%) during 5 min following this mild stress. The freezing behavior observed in *mdx52* mice is reminiscent of the innate antipredator behavior expressed by mice when confronted by fearful stimuli, suggesting that *mdx52* mice express a pathological increase of unconditioned fear-related behaviors. In the tcDNA-Ex51-treated *mdx52* mice, the freezing response was significantly reduced ($p = 0.0017$) compared with the control group (∼60% instead of 85%). TcDNA-Ex51-treated *mdx52* mice also displayed an apparently higher mobility in the recording area (Figure 2E), yet the distance traveled was not significantly improved ($p = 0.2727$,

**Figure 2. Effect of a partial restoration of Dp427 on mdx52 mice emotional reactivity**

(A) Schematic representation of the study design showing the sample sizes, the age at i.c.v. injection, the post-injection delay at which behavioral testing was initiated (7 weeks), starting with anxiety testing in the elevated plus maze and light/dark choice tests, then quantification of the unconditioned fear response (24-h intervals between tests), and finishing by auditory-cued fear conditioning 8 days later the animals were sacrificed 24 h after the last behavioral testing day and brain structures (cerebellum, hippocampus, and cortex) and spinal cord were harvested. Wild-type littermates were injected i.c.v. with saline (WT) and mdx52 mice with 400 μg of control tcDNA-sense (mdx52-sense) or tcDNA-Ex51 (mdx52-tcDNA). (B) Number of entries and time spent in the open arms of the elevated plus maze, expressed as percent of total arm entries. (C) Number of entries and time spent in the lit box (s) in the light/dark choice test. Results are mean ± SEM; *$p < 0.05$, **$p < 0.01$; Kruskal-Wallis test followed by Dunn's post-hoc tests. (D) Unconditioned fear expressed as percent time spent in tonic immobility during a 5-min period of observation following a brief scruff restraint (15 s) (mean ± SEM; **$p < 0.01$, ***$p < 0.005$; one-way ANOVA followed by Sidak post-hoc tests. (E) Representative tracking plots during the unconditioned fear test. (F) Auditory-cued fear conditioning. Performance during conditioning (fear learning) and memory retention sessions (fear retention at a 24-h post-conditioning delay) is expressed as the percent time spent freezing during presentation of the conditioned stimulus (tone, 30 s), which was repeated five times during conditioning (CS 1–5; each was an 80 dB tone lasting 30 s, followed by a foot shock) and repeated four times (CS 1–4) during the retention session performed 24 h later in a new context (tone delivered alone; no foot shock). Results are mean ± SEM; **$p < 0.01$, ****$p < 0.001$ analyzed by two-way ANOVAs.

tcDNA-Ex51 vs. sense controls) (Figure S5A). These results indicate that tcDNA-Ex51 treatment and the associated partial restoration of Dp427 lower the fearfulness induced by a mild stressful event in *mdx52* mice.

Before being submitted to the fourth and last test, all mice were gently handled for a week to minimize their basal stress level. Auditory-cued fear conditioning involves learning of an aversive cue-outcome association. The conditioned fear learning and memory performances were expressed as the percent time spent freezing during presentation of the tone (conditioned stimulus, or CS) that predicts the electric shock (unconditioned stimulus, or US). This performance was analyzed during the habituation period and during the acquisition (fear learning) and retention sessions (24 h later) comparing the tcDNA-Ex51-treated *mdx52* mice with control *mdx52-sense* mice and untreated WT littermates (Figure 2F). Importantly, freezing was low in both genotypes during the initial habituation phase that preceded acquisition (Figure 2F, left panel), while strong freezing responses were conversely observed in all mice following delivery of the electrical foot shocks (Figure S6A, Kruskal-Wallis p value = 0.614). In contrast, freezing during presentation of the auditory tone (CS) progressively increases across trials, thus reflecting learning of the predictive value of CS, i.e., the CS-US association. This was typically observed in the WT mice (Figure 2F, left panel). In contrast, acquisition of fear conditioning was clearly impaired in the control *mdx52-sense* group (Figure 2F), as they exhibited a strongly reduced conditioned freezing response compared with WT ($p = 0.0090$) during presentation of the CS (group effect: $F(2,26) = 8.137$, $p = 0.0018$). In contrast, the conditioned freezing response displayed by the tcDNA-Ex51-treated *mdx52* mice was similar to the WT group ($p = 0.5464$). The deficit in learning the predictive value of the CS observed in the untreated group of *mdx52* mice was observed during the whole learning period (group × time interaction: $F(10,130) = 1.426$, $p = 0.1756$), a result consistent with our previous study, while tcDNA-Ex51 and partial rescue of Dp427 fully restored the performance of treated *mdx52*mice to WT level.

Twenty-four hours later (retention session, Figure 2F, right panel), the control *mdx52-sense* mice showed a lower amount of freezing during the habituation phase (before CS1 delivery), which might reflect poor memory of the events experienced on the previous day. Accordingly, they also exhibited reduced quantities of freezing during the four presentations of the CS alone (not followed by electric foot shocks) (group effect: $F(2,26) = 13.47$, $p < 0.0001$), thus showing impaired fear memory. It is noteworthy that the control group (*mdx52*-sense) in this study shows a stronger memory deficit compared with our previous study.[10] The major difference between the two studies is that mice of the present study have experienced intracranial surgery, which is not a trivial factor, but instead is known to potentially modify mouse behavior. To consider this parameter all groups (WT, treated and control *mdx52*) underwent the surgery in similar conditions. These results suggest that the impact of surgery was more harmful in *mdx52* mice than in WT and treated *mdx52* mice. In contrast, tcDNA-Ex51-treated *mdx52* displayed a significantly higher performance (more freezing) compared with untreated mice ($p = 0.0415$), and this performance was similar to WT levels ($p = 0.1306$). However, performance evolution appears different (group × time interaction: $F(8,104) = 2.668$, $p = 0.0102$), in particular in response to the first conditioning stimulus (CS1) (tone not followed by electric foot shock), since WT displayed a stronger freezing response ($p = 0.0187$).

In addition, these animals were also tested in the same apparatus for contextual fear memory and showed no impairment for this type of fear-related memory (Kruskal-Wallis, $p = 0.8474$) (Figure S6B), consistent with previous work on the *mdx* mouse model.[11,25] This further confirms that *mdx52* mice are selectively impaired in their capacity to learn the Pavlovian CS-US association during auditory-cued fear conditioning.

### Partial restoration of Dp427 associated to the behavioral rescue in tcDNA-Ex51-treated *mdx52* mice

To evaluate whether these improvements in emotional-related behaviors were in line with the molecular effects of the treatment, we analyzed the different brain regions of treated mice for tcDNA biodistribution, exon 51 skipping levels, and Dp427 restoration at the end of the behavioral testing period. All groups of mice were therefore analyzed 9 weeks after the i.c.v. administration (24 h after the last behavioral test). Substantial amounts of the tcDNA-Ex51-ASO in the different brain regions was confirmed by fluorescent hybridization assay at this post-administration delay and revealed a homogeneous distribution of the ASO across the CNS ($p = 0.5786$) (Figure 3A). We also confirmed presence of the tcDNA-Ex51 in the hippocampus, cortex, and cerebellum by *in situ* hybridization (ISH) using a complementary probe in tissue sections. We clearly detected the tcDNA-Ex51 in the cerebellum, the CA1 hippocampus region, and the cortex (Figures 3B and S7A). However, it was not detected in the lateral nuclei of the amygdala, such as BLP, LaVm, and LaVL, nor in the striatum (CPu). Interestingly, we detected a tcDNA-Ex51 signal in surrounding regions: low levels in the medio- and centrolateral nuclei of the amygdala (BMP and CeL) and most tcDNA detected was found in the piriform cortex and the amygdalo-hippocampal area (Figure S7B).

Accordingly, qRT-PCR revealed approximately 15% of exon 51 skipping in the cerebellum, hippocampus, cortex, and the cervical part of the spinal cord (structure effect, $p = 0.1275$) (Figure 3C).

To further investigate the localization of the skipped and unskipped mRNA in the brain, we performed *in situ* hybridization using BaseScope duplex probes against exon junctions 50-51 (unskipped mRNA) and 50-53 (exon 51-skipped mRNA in *mdx52*). We successfully detected the exon 51-skipped mRNA in the brain of tcDNA-treated mice (turquoise dots in Figure 3D), while only the unskipped mRNA (red dots) was detected in sense-treated *mdx52* mice. We detected particular high expression of the *Dmd* transcript in the Purkinje cell layer of the cerebellum and in the CA1 hippocampal region, while dots in the cortex were relatively sparse. By quantifying the

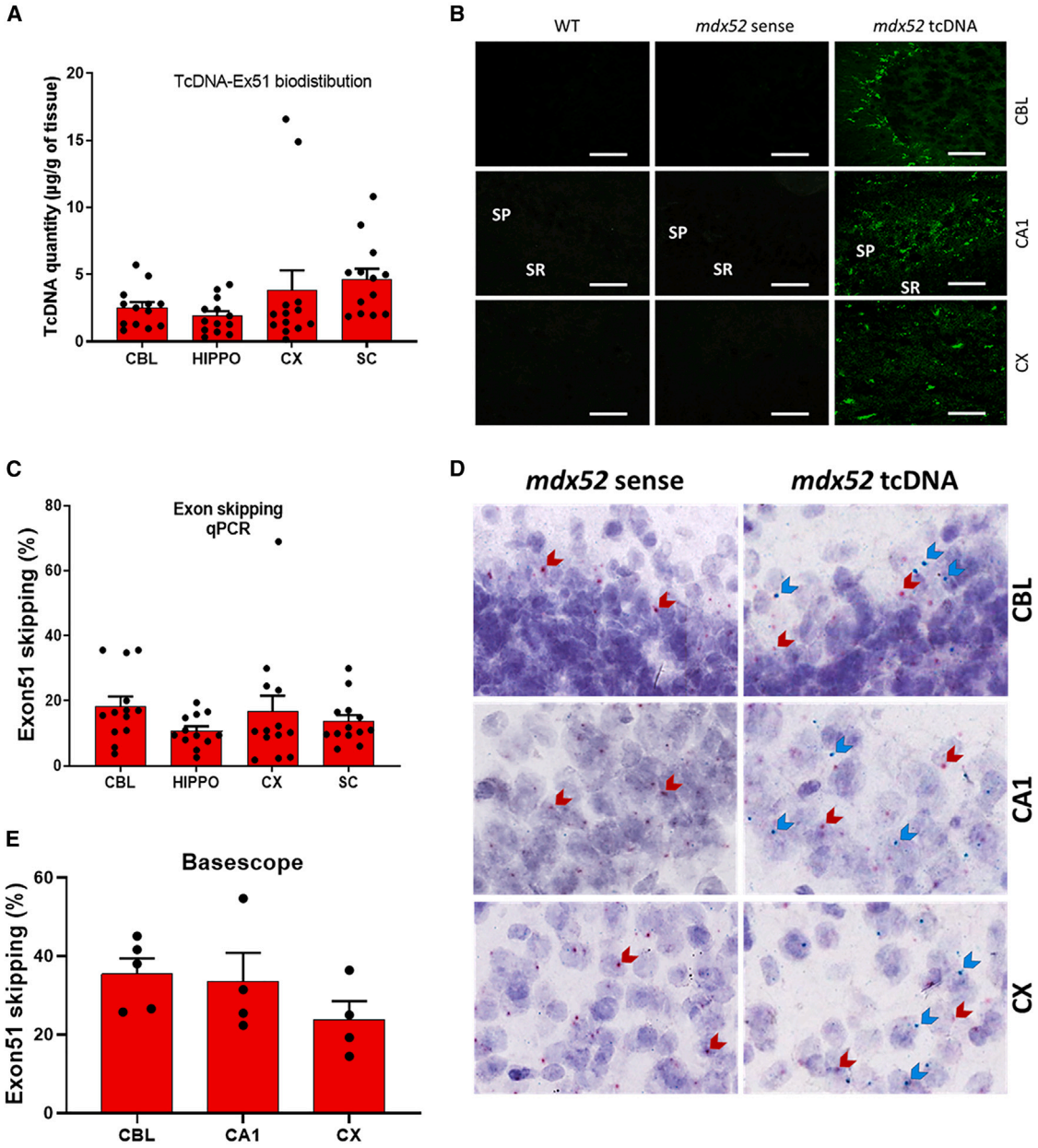


**Figure 3. Detection of tcDNA-Ex51 ASO and skipped *Dmd* mRNA 9 weeks after the i.c.v. injection of tcDNA-Ex51 in *mdx52* mice**

(A) Quantification by fluorescent hybridization assay of tcDNA-Ex51 content in various CNS tissues (CBL, cerebellum; HIPPO, hippocampus; CX, cortex; SC, the cervical part of the spinal cord) 9 weeks after the i.c.v. administration. Results are expressed as mean ± SEM; n = 13 *mdx52*-tcDNA-Ex51. (B) Detection of tcDNA-Ex51 in different brain regions (CBL, cerebellum; CX, cortex; and CA1 of the hippocampus) by fluorescent *in situ* hybridization. (C) Quantification of exon 51-skipping levels by qRT-PCR in the same tissues as above 9 weeks after i.c.v. administration (mean ± SEM; n = 13 mice per group). (D) Detection of skipped dystrophin mRNA using the BaseScope hybridization technology in the CBL, CA1 region of the hippocampus, and the CX of control-treated (*mdx52* sense) and tcDNA-Ex51-treated *mdx52* mice (*mdx52* tcDNA). BaseScope probes were directed against the exon 50-51 junction for the native (full) mRNA (red dots indicated with red arrows) and against the exon 50-53 junction for exon 23-skipped mRNA only detected in tcDNA-Ex51-treated *mdx52* mice (turquoise dots, indicated with blue arrows). Dark blue/purple elements are counterstained nuclei. (E) Percentage of exon 51-skipped mRNAs in the different brain regions, calculated as the total surface covered by turquoise staining (skipped mRNA) normalized to total (red + turquoise) staining (skipped and unskipped mRNA (mean ± SEM; n = 4 mice per group).

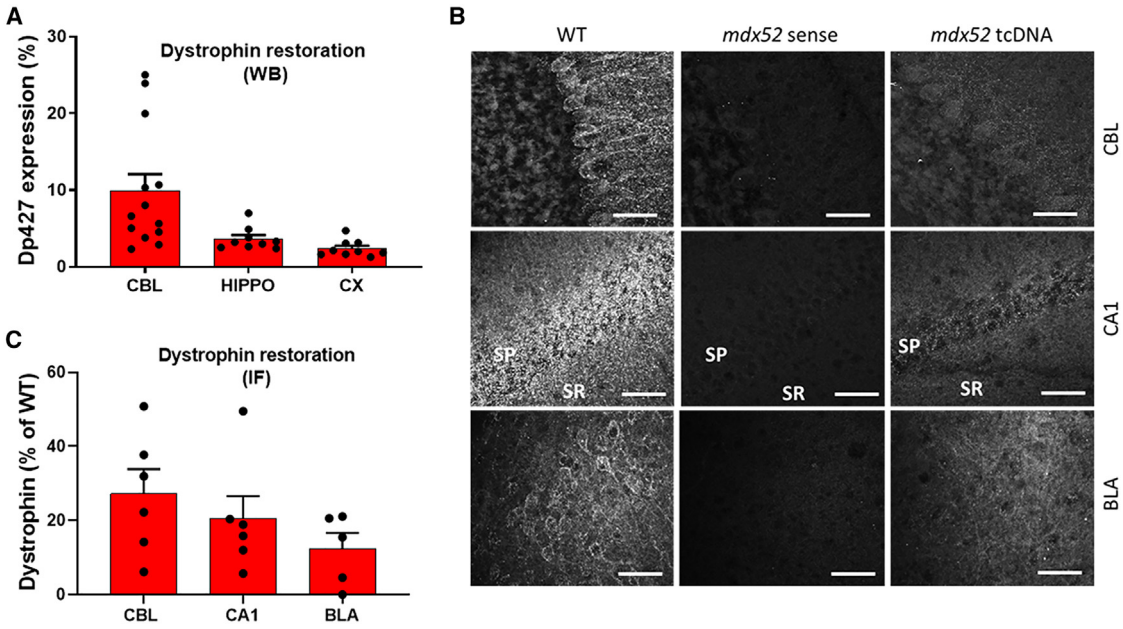


**Figure 4. Partial restoration of Dp427 associated to the behavioral rescue in tcDNA-Ex51-treated *mdx52* mice**

(A) Quantification of dystrophin protein restoration by western blot in different brain regions (CBL, cerebellum; HIPPO, hippocampus; CX, cortex) 9 weeks after i.c.v. administration. (B) Detection of the restored dystrophin protein by immunofluorescence in the Purkinje cell and molecular cell layers of the cerebellum, in the stratum pyramidal (SP) and proximal stratum radiatum (SR) of the CA1 region of the hippocampus, and in the basolateral nucleus of the amygdala (BLA) of WT and *mdx52* mice 9 weeks after the i.c.v. administration of tcDNA-sense sequence (*mdx52* sense) or tcDNA-Ex51 (*mdx52* tcDNA). Scale bars, 12 μm. (C) Quantification of dystrophin restoration detected by immunofluorescence in the different structures. Results are expressed as mean ± SEM; n = 3–6 mice per group.

relative area covered by the red and blue signals, we were able to estimate the level of exon skipping in the different brain regions. We report an average of 33.5% of exon 51 skipping in the CA1 layer of the hippocampus, 23.8% in the cortex, and 35.5% in the cerebellum (Figures 3E and S8A). Interestingly in the cerebellum, while the quantification represents the average staining across the different lobules, we were able to detect higher skipped transcripts in the lobules close to the fourth ventricle compared with more distant lobules (Figure S8B). In addition, we were also able to detect few dots corresponding to exon 51-skipped transcripts the BLA region of the amygdala (Figure S8A).

We also quantified the levels of Dp427 restoration in the various brain regions using immunoblots and found 9.9% protein levels in the cerebellum, 3.6% in the hippocampus, and 2.4% in the cortex of tcDNA-Ex51-treated *mdx52* mice (ANOVA $p = 0.0004$, CBL vs. HIP $p = 0.0019$, CBL vs. CX $p = 0.001$, HIP vs. CX $p = 0.9743$) (Figures 4A and S9). No Dp427 was detected in skeletal muscles (data not shown), indicating no peripheral effect after i.c.v. delivery. We also checked the expression of Dp140, the re-expression of which following treatment was not expected since skipping of exon 51 should remove the start codon of Dp140. Our results confirmed the absence of Dp140 in both control- and tcDNA-treated *mdx52* mice (Figure S10).

Finally, we determined the localization of the restored Dp427 using immunofluorescence techniques and the DYS-1 antibody directed against the N terminus of the dystrophin protein (Figure 4B). This revealed approximately 25% of Dp427 restoration in the cerebellum (in both the PCL and MCL) and 20% in the CA1 region (in SP and SR layers) of the hippocampus, in line with the distribution of the tcDNA and skipped mRNA. Moreover, we found approximately 12% of Dp427 expression in the basolateral nucleus of the amygdala (Figure 4C).

Altogether, these results indicate that administration of tcDNA-Ex51 in the lateral ventricles of *mdx52* mice induces exon 51 skipping and a partial restoration of Dp427 in the cerebellum, hippocampus, and cortex of treated mice. This postnatal restoration in the range of 3%–10% of WT levels partially rescued the emotional-related deficits in this mouse model. Yet, we noticed that some parameters analyzed during the fear response (such as distance traveled shown in Figure S5A) were not rescued by the partial restoration of Dp427 in the CNS. This is intriguing given that we have previously shown that a low level of Dp427 restoration in the CNS (in the range of 2%) following systemic delivery of tcDNA-ASO could lead to the correction of the abnormal restraint-induced fear response in *mdx* mice.[20–22] This raises questions about the involvement of the peripheral system, including skeletal and cardiac muscles, in this deficit. To further investigate this aspect and evaluate whether rescue of Dp427 in the periphery could improve the partial rescue in the restraint-induced fear response, we performed combined intravenous and central treatments.

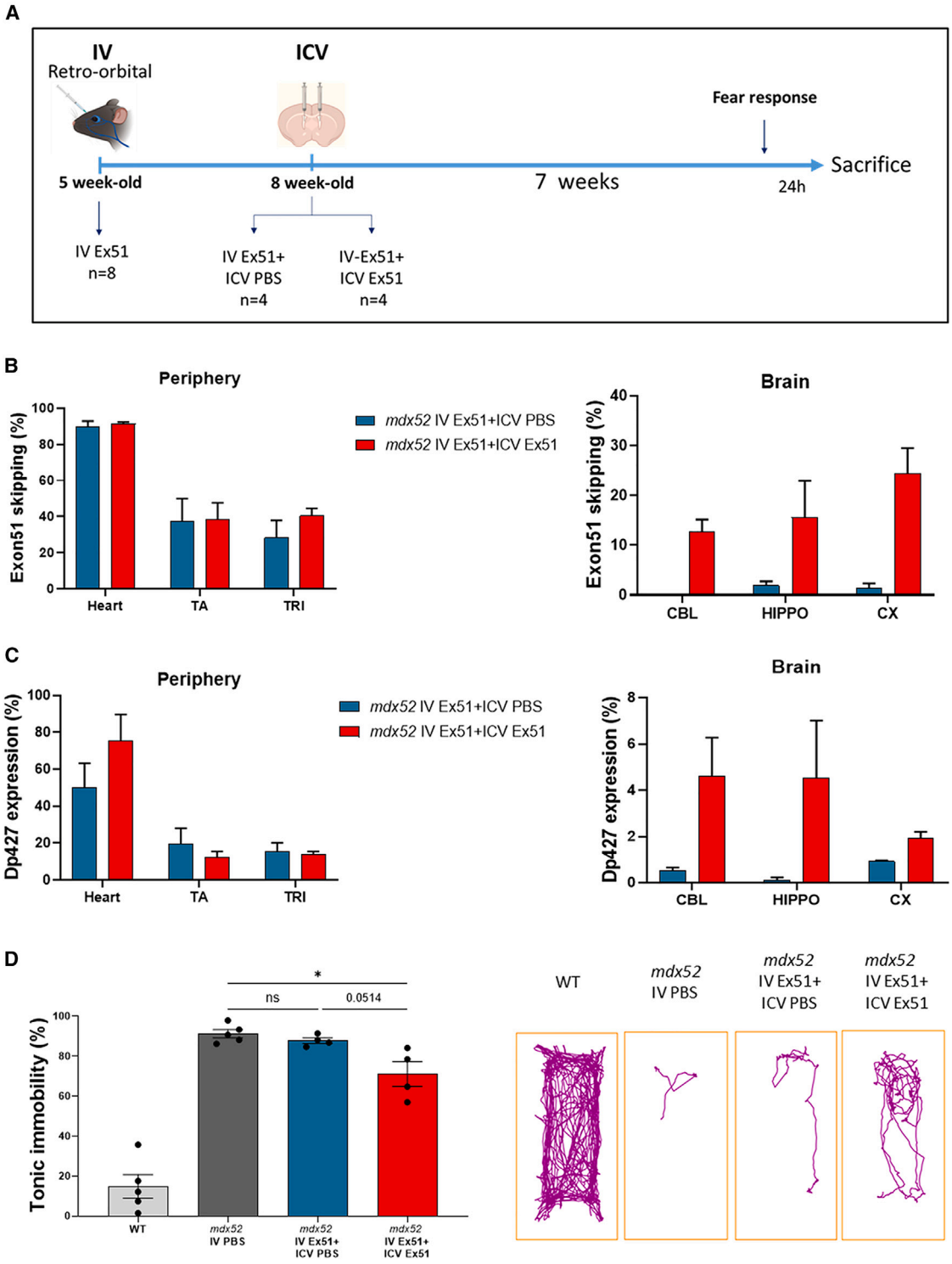


**Figure 5. Combined restoration of Dp427 in muscles and brain using i.v. injection of AAV-U7-Ex51 and i.c.v. injection of tcDNA-Ex51**

(A) Schematic representation of the study design showing the sample sizes, the time of i.v. and i.c.v. injections, and the post-injection delay at which fear response was assessed (7 weeks post-i.c.v.). (B) Quantification of exon 51-skipping levels by qRT-PCR in peripheral tissues (heart; TA, tibialis anterior; TRI, triceps) and brain tissues (CBL,

*(legend continued on next page)*

### Combined restoration of Dp427 in muscles and brain

We combined a systemic treatment using the previously described AAV-U7snRNA system[18,26] with the i.c.v. injection of tcDNA-Ex51. The experimental design is represented in Figure 5A. A group of 5-week-old *mdx52* mice was first injected intravenously with scAAV9-U7Ex51, which has been shown to rescue Dp427 expression in muscles and heart, but not in the brain.[18] Half of these systemically treated *mdx52* mice also received an i.c.v. injection of tcDNA-Ex51 3 weeks later (group named i.v. Ex51 + i.c.v. Ex51, n = 4), while the other half received an i.c.v. injection of saline (group named i.v. Ex51 + i.c.v. PBS, n = 4). Groups of control *mdx52* mice (n = 5, only injected i.v. with PBS) and WT mice (n = 5) were also included in the study. Brain and muscle tissues were analyzed 7 weeks after the i.c.v. injection, which corresponds to approximately 10 weeks after the intravenous delivery of AAV, when mice were aged 15 weeks.

Exon 51 skipping levels were measured both in the CNS and in the periphery following both types of treatment (i.v. Ex51 + i.c.v. PBS or i.v. Ex51 + i.c.v. Ex51). We detected similar levels of exon 51 skipping in the periphery after both treatments, with up to 95% of exon skipping in the heart and ∼40% in the tibialis anterior (TA) and triceps (TRI) (Figure 5B), confirming the peripheral effect of the AAV-U7Ex51 with no additional effect of the subsequent i.c.v. administration (treatment effect, p = 0.5224). In contrast, and as expected, exon 51 skipping levels in the CNS were much higher (treatment effect, p = 0.0033) when the initial i.v. injection of scAAV9-U7Ex51 was followed by the i.c.v. injection of tcDNA-Ex51. Exon 51 skipping was relatively homogeneous in the different regions (structure effect, p = 0.228) in the *mdx52* mice that received the i.c.v. injection of tcDNA-Ex51, as observed previously (Figures 1B and 3C). This was in line with the distribution of tcDNA-Ex51 in the different brain regions (p = 0.4451) (Figure S11). Western blot analysis also revealed comparable restoration levels of the Dp427 protein in the periphery in both treatment groups (treatment effect, p = 0.5774), reaching about 50% of WT levels in the heart and 15% in the TA and the TRI (Figure 5C). In the CNS, 3%–10% of Dp427 expression was detected in the different brain regions of the i.v. Ex51 + i.c.v. Ex51 group, while less than 1% was detected in the i.v. Ex51 + i.c.v. PBS group. These analyses confirmed that the i.v. Ex51 + i.c.v. PBS group displayed mostly Dp427 restoration in the periphery, while the combined i.v. Ex51 + i.c.v. Ex51 group displayed Dp427 both in the periphery and in the CNS.

The fear response was assessed in these mice and is shown in Figure 5D. A representative tracking plot for each group illustrates the mice mobility following the different treatments. The fear response of the i.v. Ex51 + i.c.v. PBS group was not different from the i.v. PBS (p = 0.5933), suggesting that postnatal peripheral rescue of Dp427 had no impact on this phenotype. In contrast, the i.v. Ex51 + i.c.v. Ex51 group showed significantly lower freezing amount after acute stress induction compared with the i.v. PBS group (p = 0.0203) and this was also marginally significant compared with the i.v. Ex51 + i.c.v. PBS group (p = 0.0514) (Figure 5D). This confirms our previous results indicating that partial restoration in the CNS had a positive effect on the fear response. Importantly, however, the amount of freezing in the i.v. Ex51 + i.c.v. Ex51 group was not statistically different from *mdx52* treated with i.c.v. Ex51 only, as shown in Figure 2D (∼60% of freezing) (p = 0.3645). Similarly, the distance traveled (Figure S4B) was not significantly improved in the i.v. Ex51 + i.c.v. Ex51 group compared with controls (p = 0.9240), as previously shown for i.c.v. only (Figure S5A). These results indicate no significant cumulative effect of the peripheral rescue of Dp427 over a partial central restoration on the fear response rescue in *mdx52* mice.

## DISCUSSION

Cumulative loss of centrally expressed dystrophin proteins (Dp427, Dp260, Dp140, and Dp71) is associated with more severe emotional and cognitive deficits in DMD patients.[1,9] The *mdx52* mouse model (lacking Dp427, Dp260, and Dp140) is therefore a useful model to investigate brain comorbidities in DMD and their potential reversibility. We previously confirmed that *mdx52* mice that carry a mutation profile frequently found in DMD patients display more severe phenotypes than *mdx* mice that only lack Dp427.[10] In particular, *mdx52* mice display enhanced anxiety and a severe impairment in learning an amygdala-dependent Pavlovian association. In this context, we aimed to evaluate an exon-skipping approach targeting the dystrophin exon 51, which is expected to selectively restore Dp427 expression in this model. DMD patients amenable to exon 51 skipping represent the largest patient group eligible for exon skipping therapy, i.e., approximately 13% of DMD patients.[27] The PMO ASO eteplirsen was the first approved drug for the treatment of DMD in the US in 2016.[28] However, since exon 51 contains the initiation codon for Dp140, the exclusion of this exon can only rescue Dp427 (and Dp260 expressed in the retina).

In this study, we investigated the impact of Dp427 restoration on CNS alterations in the *mdx52* model. For that purpose, *mdx52* mice were treated with the maximal feasible dose (400 μg) of tcDNA-Ex51 in the lateral brain ventricles. We first showed that tcDNA-Ex51 was homogenously distributed in the different brain regions following i.c.v. injection, inducing approximately 20%–30% of transcripts skipped for exon 51. Interestingly, the half-life of tcDNA in brain regions was longer than what we had previously reported in skeletal muscles

cerebellum; HIPPO, hippocampus; CX, cortex) 7 weeks after the i.c.v. administration. Results are expressed as mean ± SEM; n = 4 mice per group. (C) Quantification of Dp427 protein levels by western blot in peripheral tissues (heart; TA; TRI) and brain tissues (CBL; HIPPO; CX) 7 weeks after i.c.v. administration. Results are expressed as mean ± SEM; n = 4 mice/group. (D) Restraint-induced unconditioned fear responses expressed as the percent time spent freezing (left panel) and representative tracking plots (right panel) for each group. *Mdx52* mice were injected i.v. when they were 5 weeks old with PBS (*mdx52* i.v. PBS) or with AAV-U7Ex51, then i.c.v. at 8 weeks old with PBS (*mdx52* i.v. Ex51 + i.c.v. PBS) or Ex51tcDNA-Ex51 (*mdx52* i.v. Ex51 + i.c.v. Ex51) and compared with WT littermates (WT). Results are expressed as mean ± SEM; n = 4 mice/group.

after systemic delivery,[22] where only about 10% of ASO was found left in tissues 12 weeks after the end of the treatment. More importantly exon skipping levels were found to be very stable between 3 and 11 weeks after the injection, which is in line with previous reports indicating a particularly long lasting effect of ASO in the CNS.[29] Dp427 protein expression, ranging from 5% to 10% in the different brain regions appeared stable between 7 and 11 weeks after the i.c.v., which determined the optimal therapeutic window to investigate treatment effect on the behavioral phenotypes found to be impaired in this mouse model.

To evaluate the impact of Dp427 rescue on behavioral phenotypes, groups of *mdx52* mice received either a tcDNA targeting exon 51 or a control tcDNA sense sequence, and their WT littermates received saline to take the surgery bias into consideration. The animals were successively submitted to a selection of tests in which *mdx52* mice display strong deficits. Anxiety was the first central disturbance analyzed using two distinct behavioral tests. We found that treatment with tcDNA-Ex51 fully compensated the anxiety phenotype measured in the elevated plus-maze test, while emotional reactivity was only partially improved in the light/dark choice test. Interestingly, we noticed that all injected mice displayed more anxiety compared with non-injected mice in our previous study.[10] The differences between WT and control *mdx52* were also lower in this study, suggesting a potential effect of the surgery, which might have partially masked or attenuated the treatment efficacy. The third test performed was the unconditioned fear response. This is one of the main behavioral outcomes in *mdx52* mice, which likely reflects a maladaptive response to mild stress and enables to measure their pathological stress reactivity. Treatment with tcDNA-Ex51 induced a significant reduction of the fear response in *mdx52* mice, despite a large variability observed between individuals. An additional parameter, the distance traveled, measured during this test, was not significantly improved, indicating a partial recovery improvement. Finally, we evaluated the effect of treatment on mouse performance in the auditory-cued fear conditioning, in which *mdx52* mice display robust impairments in acquiring and recalling fear memories. We show that treatment rescues acquisition of this Pavlovian associative learning and partially improves the recall of fear memory. This suggests that low restoration of brain Dp427 was sufficient to compensate the learning deficits but was insufficient to fully overcome the fear memory deficits during fear conditioning. These findings contrast with those reported previously in *mdx* mice with a mutation in exon 23 (hence only lacking Dp427), in which partial Dp427 restoration only slightly improved fear memory but had no effect on fear learning.[24] One possible explanation may be the localization of the restored Dp427, which appears higher in the cerebellum of *mdx52*-treated mice in this study than previously treated *mdx* mice, in which restoration was higher in the hippocampus.[24] The biodistribution of the tcDNA-Ex51 indeed appears more homogeneous across the different brain regions than in our previous study using the same dose of a tcDNA targeting the *mdx* exon 23, which may be due to sequence-specific properties of each ASO. Higher restoration of Dp427 in the cerebellum may explain this difference in fear-learning performances; indeed, recent studies showed an involvement of the cerebellum in fear-learning tasks.[30] Overall, we demonstrate that the tcDNA-Ex51 central treatment improves both the emotional reactivity and emotional learning in *mdx52* mice.

While our results are particularly encouraging for the future treatments of DMD patients, they also raise many questions related to the incomplete rescue of the phenotypes. A first hypothesis to explain this partial phenotypic rescue is that the absence of Dp140 participates in the genesis of these phenotypes, but it is not restored by postnatal exon 51 skipping. This is supported by our previous observation that anxiety is more severe in *mdx52* mice compared with *mdx* mice lacking only Dp427. However, the unconditioned fear response was not completely rescued either, although previous studies reported similarly enhanced fear responses in *mdx* and *mdx52* mice,[10,31] suggesting that this phenotype is mainly caused by the lack of Dp427. This is also supported by our previous work showing that Dp427 restoration in the brain can completely rescue the fear response in *mdx* mice.[24] The partial improvement in the fear response observed here in *mdx52* mice and the high inter-individual variability could alternatively be due to the low levels of Dp427 restored. Indeed, in this study, efficient exon 51 skipping (10%–30% across the different brain regions) only restored 3%–10% of Dp427 protein, while we demonstrated previously that a similar treatment with a tcDNA targeting exon 23 restored up to 25% of Dp427 in the hippocampus of *mdx* mice.[24] This discrepancy in dystrophin restoration between *mdx* and *mdx52* mice, which has been reported previously,[18] is not due to variable skipping efficacy between exon 23 and 51, which are relatively similar (20%–30%). Instead, it was suggested that it may be due to differences in the *Dmd* mRNA levels between *mdx* and *mdx52* models, given that the *DMD* gene is subjected to transcript imbalance, limiting the amount of transcripts available in particular in the 3′ region.[32,33] However, we have also shown previously in *mdx* mice that a systemic—intravenous—treatment with tcDNA-ASO induces only very low levels of Dp427 in the brain, but normalizes the fear response.[20]

Taking all these observations into consideration, we hypothesized that the slightly more severe muscle phenotype of *mdx52* mice compared with *mdx* mice,[34] also shown to be more severe on the C57Bl/6 genetic background,[35] could have had an impact on the fear response, which therefore could not be fully restored by intracerebral treatment only. Recent studies questioned the involvement of central and peripheral dystrophin in stressful conditions.[36–38] Razzioli et al. indeed demonstrated that transgenic *mdx* mice expressing dystrophin or utrophin in skeletal muscles display significantly lowered fear response after a scruffing-induced stress but still not to the WT level, which does not fully account for the peripheral origin of the phenotype. Moreover, by knocking out the nSMase2/Smpd3 inflammation regulatory protein in *mdx* mice, it was found that the reduced inflammation in this model was associated with a decreased fear response.[37] Lindsay et al., in line with these studies showed an activation of the hypothalamic-pituitary-adrenal axis suggesting a central involvement.[36] In parallel, previous studies showed a fully

rescued fear response following a locally central treatment in *mdx* mice confirming a strong central origin to this phenotype.[24]

The extent of skeletal muscle involvement in *mdx* mouse models (including the *mdx52* model) is relatively mild, in particular when the mice are young as in this study where the behavior is analyzed at age 3–4 months. For example, the mean duration of visits (total time spent in the lit compartment normalized to the number of visits) in the light/dark choice test was comparable between the *mdx52* group and their WT littermates (Figure S12), indicating no major hypoactivity in this mouse model. Yet, some specific parameters with higher muscular demand, such as the grip strength test, were previously shown to be significantly reduced in *mdx52* compared with *mdx* mice.[34] We therefore wondered if the absence of Dp427 in muscles and heart could contribute to the only partial rescue of the restraint-induced fear response that we observed in *mdx52* mice after treatment with tcDNA-Ex51. In the present study, we demonstrate that the peripheral restoration of Dp427 in skeletal (15% in the TA and the TRI) and cardiac (50% of WT levels) muscles using scAAV9-U7Ex51[18] does not improve the fear response on its own. Moreover, a treatment combining i.v. injection of scAAV9-U7Ex51- and the i.c.v. injection of tcDNA-Ex51 does not improve further the effect on the fear response compared with i.c.v. alone of tcDNA-Ex51. These results confirm that brain Dp427 plays a major role in the genesis of the fear response phenotype.

### Concluding remarks

Our results suggest that restoring Dp427 in the brain postnatally, even partially, can improve or at least alleviate some severe central comorbidities associated with DMD. More investigations are needed to explore the possibility to further improve the postnatal reversibility of these deficits. It would be interesting to investigate higher levels or structure-specific restoration of Dp427, such as in the amygdala, but also restoration at earlier time points (in neonates, for example) to see whether a more complete rescue could be achieved. Finally, considering that *mdx52* mice also lack Dp140 in the brain, it would be particularly insightful to investigate its restoration, either alone or in combination with Dp427, using exon 53 skipping. These future lines of research would help shed some light on the role of Dp140 and its involvement in the central functions. Yet, these findings are particularly encouraging at a time where new generations of ASO are being developed and may offer the exciting opportunity to treat both the dystrophic muscle phenotype and the brain comorbidities in DMD patients.

## MATERIALS AND METHODS

### Animals and ASOs

Exon 52-deleted X chromosome-linked muscular dystrophy mice (*mdx52* mice) were generated by the group of Dr. Katsuki Motoya.[13] It was produced by replacement of exon 52 of the *DMD* gene by the neomycin resistance gene, thereby eliminating expression of Dp427, Dp260, and Dp140 dystrophins but preserving expression of Dp116 (in peripheral nerves) and of Dp71 (in brain and retina).[13] The mouse line was backcrossed with the C57BL/6J strain for more than eight generations. The mouse line has been provided by Prof. Sasaoka Toshikuni (Department of Comparative & Experimental Medicine/Brain Research Institute; Niigata University, Japan). Breeders were provided to our lab by Dr. Jun Tanihata and Dr. Shin'ichi Takeda (National Center of Neurology and Psychiatry, Tokyo, Japan). Heterozygous females were crossed with C57BL/6JRj males to generate *mdx52* and littermate control (WT) males in the animal facility of Neuro-PSI at Saclay (France). Genotypes were determined by PCR analysis of tail DNA. Animal care and all experimental procedures complied with the European Communities Council Directive (CEE 86/609/EEC), EU Directive 2010/63/EU, French National Committee (87/848) and Ethic Committee (Paris Center et Sud, no. 59).

The tcDNA-Ex51 used in this study targets an exonic splicing enhancer within exon 51 of the dystrophin pre-mRNA (position +48 + 62) and was synthesized by SQY Therapeutics (Montigny-le-Bretonneux, France). The control tcDNA named tcDNA-sense is the complementary sequence and was therefore not hybridizing to the target dystrophin pre-mRNA. Palmitic acid was conjugated at the 5′ end of the tcDNA full phosphodiester via a C6-amino linker and a phosphorothioate bond as described previously.[22]

### Stereotaxic surgery and systemic injections

i.c.v. injections were performed in 6- to 8-week-old *mdx52* and WT littermate male mice deeply anesthetized by a single intraperitoneal injection of ketamine (95 mg/kg)/medetomidine (1 mg/kg). TcDNA-Ex51, tcDNA-sense, or saline solutions (phosphate-buffered saline, 0.1 mol/L) were injected bilaterally into the lateral brain ventricles (−0.5 mm from bregma; 1 mm lateral; −2 mm from dura).[39] A volume of 5 μL was infused in each ventricle at a rate of 0.3 μL/min. A total amount of 400 μg of tcDNA-Ex51 was thus distributed bilaterally. The systemic treatment consisted in intravenous retro-orbital injections under gaseous anesthesia (2.5% isoflurane mixed with air). A group of 5-week-old male *mdx52* mice was injected with 3 E+14 vector genomes (vg) of self-complementary adeno-associated vector serotype 9 encoding the U7snRNA engineered to target dystrophin exon 51 (scAAV9-U7Ex51M), as described previously.[18,40] Treatment of animals was pseudorandomized in each cage so that it was balanced within the litters and with comparable distribution among litters.

### Experimental groups

Siblings were kept in groups (two to five per cage) under a 12-h light-dark cycle (light on: 7.00 a.m.) with food and water *ad libitum*. For the kinetics study, groups of five mice were used, and *mdx52* mice received i.c.v. injections of either tcDNA-Ex51 or saline. The animals were sacrificed at three different time points: 3, 7, and 11 weeks after i.c.v. injection (n = 5 per time point). Brains were dissected out, one hemisphere was fresh frozen in dry ice for *in situ* analysis and the other one was dissected to isolate hippocampus (HIP), cerebellum (CBL), cortex (CX), and the cervical part of the spinal cord samples that were snap-frozen in liquid nitrogen for biodistribution, qPCR, and western blot analyses.

For the behavioral study, three groups of mice were used and underwent surgery in identical conditions. Eight-week-old *mdx52* male mice were treated with the tcDNA-Ex51 (n = 13) or with the tcDNA-sense as a control (n = 10), while WT littermate males were treated with saline (n = 13). Seven weeks after i.c.v. injections, within a therapeutic window of 2 weeks, the mice were tested in a battery of behavioral tests in the following order: elevated plus maze, light/dark choice test, and restraint-induced unconditioned fear with 24 h interval. The order of the tests was specifically chosen to minimize their influence on each other. A week of gentle handling preceded the auditory-cued fear conditioning, to reduce stress before testing. Behavioral testing was performed blind to the genotype. The experimental protocol is shown in Figure 2A. For the treatment combining systemic and central injections, a separate group of *mdx52* male mice (n = 8) underwent intravenous injections of 3 E+14 vg of scAAV9-U7Ex51M. Three weeks later, half of them also received tcDNA-Ex51 by i.c.v. and the other half received saline. Seven weeks after the i.c.v. injections, these animals and their non-injected WT littermates (n = 5) were submitted to restraint-induced unconditioned fear.

### Behavioral analysis

#### *Elevated plus-maze*

The maze had two facing arms enclosed with high walls (closed arms, 20 × 8 × 25 cm), two open arms without walls (20 × 8 cm), and a central area (8 × 8 cm) forming a plus sign situated above a vertical stand to elevate the maze 65 cm above the floor. Illumination was 150 lx in open and 30 lx in closed arms. Mice were individually placed at the center of the maze with the head facing a closed arm. The number of entries and time spent in open or closed arms were manually scored for 5 min.

#### *Light-dark choice*

The apparatus had 20-cm-high Plexiglas walls and consisted of a black and dark compartment (15 × 15 cm; illumination <15 lx) connected by a trap door (6 × 6 cm) to a brightly lit white compartment (40 × 15 cm). Bright illumination was provided by a light source placed at the end of the white compartment, opposite from the trap door to create an illumination gradient (50 lx close to the trap door to 600 Lx close to the light), as described previously.[10] Each mouse was placed in the dark compartment for 10 s, the trap door was then open, and the mouse allowed to freely explore the whole apparatus for 5 min. Step through latency, number of entries, and total time spent in the lit compartment were manually scored by the experimenter.

#### *Restraint-induced unconditioned fear*

The mouse was restrained by grasping the scruff and back skin between thumb and index fingers, while securing the tail between the third and little fingers and tilting the animal upside-down in order that the ventral part of its body faced the experimenter. After 15 s, the mouse was released to a novel cage (24 × 19 cm, with 12-cm-high walls) containing clean sawdust and then video-tracked for 5 min under dim illumination (60 lx) using the Any-maze software (Stoelting). Unconditioned fear responses induced by this short acute stress were characterized by periods of tonic immobility (freezing) and quantified during a 5-min recording period. Complete immobilization of the mouse, except for respiration, was regarded as a freezing response.[41] The percent time spent freezing was calculated for group comparisons.

#### *Auditory-cued fear conditioning*

The conditioning procedure was carried out using the StartFear system (Panlab, Barcelona) under the same conditions previously used in our studies of *mdx* and *mdx52* mice.[10,11] The conditioning chamber (25 × 25 × 25 cm) had three black methacrylate walls, a transparent front door, a grid floor connected to a shock scrambler to deliver unconditioned stimuli (US), and a speaker mounted on the ceiling to deliver audible tones as conditioned stimuli (CS). The conditioning chamber rested on a high sensitivity weight transducer system to generate an analog signal reflecting animal's movement. The chamber was confined in a ventilated soundproof enclosure (67 × 53 × 55 cm) on an anti-vibration table with a surrounding 60-dB white noise. Interchangeable floors and walls (i.e., plain floor and white walls) were used to analyze retention of cued fear in a novel context. On the first day (acquisition), a 2-min baseline period (habituation "H") was recorded before delivery of five CS–US pairs (tone [CS], 80 dB, 10 kHz, 30 s; footshocks [US], each at 0.4 mA for 2 s) with variable and pseudo-randomly distributed intervals between pairs of stimuli (60, 120, and 180 s). On the next day (retention), the session started by placing the mouse in a different context for 2 min (H) before delivery of four CS (80 dB, 10 kHz, 30 s) separated by intervals of variable durations (60, 90, and 120 s). Animals' movements were sampled at 50 Hz for quantitative analysis (FREEZING software, Panlab). Freezing was measured during delivery of the CS (periods of 30 s) to specifically reflect associative learning performance.[42]

### tcDNA tissue quantification by fluorescent hybridization assay

Tissues were homogenized using the Precellys 24 (Bertin Instruments, France) in lysis buffer (100 mmol/L Tris-HCl [pH 8.5], 200 mmol/L NaCl, 5 mmol/L EDTA, 0.2% sodium dodecyl sulfate) containing 2 mg/mL of proteinase K (Invitrogen) (50 mg tissue/mL of buffer), followed by incubation overnight at 55°C in a hybridization oven. After centrifugation at 14,000 rpm (Sorval ST 8R centrifuge, 75005719 rotor) for 15 min, the supernatant was used in the assay. Quantification of tcDNA was performed using a hybridization assay with a molecular beacon probe as described previously.[43] in brief, 10 μL of tissue lysates was incubated with a 5′ Cy3-DNA complementary probe conjugated with HBQ quencher at 3′ in a black non-binding 96-well plates (Thermo Fischer Scientific); PBS was added to a final volume of 100 μL per well and fluorescence was measured on a spectrophotometer (Ex 544 nm/Em 590 nm using FluoStar Omega). The amount of tcDNA in tissues was determined using a standard curve build on the measurement of known tcDNA quantities dissolved in the respective tissue lysates of saline-treated animals.

### RNA analyses

Total RNA was isolated from dissected brain structures using TRIzol reagent according to the manufacturer's instructions (Thermo Fisher

Scientific). For visualization of exon-skipping efficacy on gels, aliquots of 1 μg of total RNA were used for RT-PCR analysis using the Access RT-PCR System (Promega) in a 50-μL reaction using the external primers Ex49F (5′-AAACTGAAATAGCAGTTCA AGC-3′) and Ex 53R-Aoki (5′- ACCTGTTCGGCTTCTTCCTT-3′). The cDNA synthesis was carried out at 55°C for 10 min, followed by the PCR of 30 cycles of 95°C (30 s), 58°C (1 min), and 72°C (1 min). PCR products were analyzed on 1.5% agarose gels.

Exon 51 skipping was also measured by TaqMan quantitative PCR as described,[18] using a TaqMan assays designed against the exon 50-51 junction (assay Mm.PT.58.41685801: forward: 5′-CAAAGCAGCCT GACCGT-3′; reverse: 5′-TGACAGTTTCCTTAGTAACCACAG-3′; probe: 5′-TGGACTGAGCACTACTGGAGCCT-3′) and the exon 50-53 junction (forward: 5′- GCACTACTGGAGCCTTTGAA-3′; reverse: 5′- CTTCCAGCCATTGTGTTGAATC-3′; probe: 5′-ACAG CTGCAGAACAGGAGACAACA-3′) (Integrated DNA Technology). One hundred and fifty nanograms of cDNA was used as input per reaction and all assays were carried out in triplicate. Assays were performed under fast cycling conditions on a Bio-Rad CFX384 Touch Real-Time PCR Detection System, and all data were analyzed using the absolute copy number method. For a given sample, the copy number of skipped product (exon 50-53 assay) and unskipped product (exon 50-51 assay) were determined using the standards Ex49-54Delta52 and Ex49-54Delta51 + 52, respectively (gBlocks gene fragments from Integrated DNA technology). Exon 51 skipping was then expressed as a percentage of total dystrophin transcripts (calculated by the addition of exon 50-51 and exon 50-53 copy numbers).

### Western blot analyses

Protein extracts were obtained from brain structures treated with RIPA lysis and extraction buffers (Thermo Fisher Scientific) complemented with SDS powder (5% final) (Bio-Rad, France). Total protein concentration was determined with the BCA Protein Assay Kit (Thermo Fisher Scientific). Samples were denatured at 100°C for 3 min and 25 μg of protein was loaded onto NuPAGE 3%–8% Tris-acetate protein gels (Invitrogen), following the manufacturer's instructions. Dystrophin protein was detected by probing the membrane with NCL-DYS1 primary monoclonal antibody (NCL-DYS1; Novocastra, Newcastle, UK) and vinculin was detected as an internal control with the hVin-1 primary antibody (Sigma), followed by incubation with a goat anti-mouse secondary antibody (IRDye 800CW Goat anti-mouse IgG, Li-Cor, Germany). Bands were visualized using the Odyssey CLx system (Li-Cor). The quantification was done using the Empiria Studio software (Li-Cor) after normalization to internal control (vinculin) and based on a standard curve specific to each brain structure and made of a mix of WT and *mdx52* control lysates to obtain defined percentages of dystrophin (0%, 5%, 10%, and 20% of corresponding WT tissues).

### *In situ* analysis of brain sections

Brain fresh-frozen 30-μm-thick cryosections were collected onto Superfrost+ slides and then stored at −80°C. Prior to all *in situ* analyzes, the slices were post-fixed for 5 min in a bath of acetone/methanol (1:1) at −20°C.

#### *Biodistribution*

The tcDNA distribution in the brain structures was assessed using a complementary probe conjugated to a biotin. The probe was then revealed with a streptavidin, Alexa Fluor 555 conjugate (Thermo Fisher Scientific). Images were taken at equivalent locations and exposure times using a laser scanning confocal microscope (Zeiss LSM 700, ×40 objective). Stacks of 9 to 11 images (1,024 × 1.024 pixels) spaced by 1 μm were recorded at a magnification of 156 nm/pixel. Scan tiles images (1,024 × 1,024 pixels) were taken using the ScanR Olympus HCS microscope, ×40 objective).

#### *BaseScope analyses of Dmd mRNA*

The BaseScope Duplex assay from Advanced Cell Diagnostics was used to detect the specific *Dmd* mRNA by ISH. Fresh frozen sections prepared as above for immunofluorescence were fixed in cold neutral buffered formalin and dehydrated in ethanol baths (50%, 70%, and 100%). The hydrogen peroxide, protease i.v. treatment, and RNA ISH were performed using the BaseScope Duplex reagent kit (323800, Advanced Cell Diagnostics) according to manufacturer's instructions. Specific BaseScope probes were designed against the exon 50-51 junction to detect unskipped mRNA, and against the exon 50-53 junction to specifically detect exon-51-skipped mRNA in *mdx52*. Control probes targeting peptidylprolyl isomerase B and ubiquitin C were used in parallel as positive controls, and against the bacterial dihydrodipicolinate reductase as a negative control (data not shown). At the end of the ISH, tissues were counterstained with hematoxylin Gills I (GHS132-1L, Sigma) diluted at 50% in water (30 s staining) and ammonium hydroxide 28–30 wt % (205840025, Acros Organics) diluted at 0.02% in water (30 s staining). Slides were then dried at 60°C for 45 min and mounted in Vectamount (321584, Advanced Cell Diagnostics). Images were obtained using the aperio AT2 scanner (Leica) (zoom 40×) and analyzed with ImageScope software (Leica). Signal quantification was performed in coronal sections from three mice per group at bregma −2.0 mm[39] from images taken along the hippocampal Ammon's horn (3,500 μm along CA1 and 1,100 μm along CA3), in the primary and secondary visual cortices above the hippocampal dentate gyrus in the same sections, as well as along the cerebellar Purkinje cell layer (4Cb, 5Cb, and 9Cb lobules) from sagittal sections (lateral 0.60 mm). Discrimination of specific signals was achieved by detection of turquoise staining (corresponding to the exon 50-51 junction) with a Hue value = 0.35 and color saturation threshold = 0.2, and red staining (corresponding to the exon 50-53 junction) with a Hue value = 0.5 and color saturation threshold = 0.14. The positive Pixel Count v.9 program of the ImageScope software was used for semiquantitative analysis of the relative area covered by each signal (rather than dot counts because of the variability in dot size).

#### *Immunostaining*

For Dp427 staining, slices were incubated first in a blocking solution for 90 min (10% normal goat serum, 0.3% Triton X-100, 1% BSA, and

10% FAB) at room temperature (RT), then overnight at 4°C with a monoclonal anti-dystrophin primary antibody (DYS1 Leica; dilution, 1/3 in 10% normal goat serum, 1% BSA), washed in PBS, and then incubated with secondary antibody Alexa 647 (1:500, 45 min, RT). Controls prepared by omitting the primary antibody showed no specific staining. Images were taken at equivalent locations and exposure times using a laser scanning confocal microscope (Zeiss LSM 700, ×40 objective). Stacks of 9 to 11 images (1,024 × 1,024 pixels) spaced by 1 μm were recorded at a magnification of 156 nm/pixel. Quantification of Dp427 re-expression in the CA1 hippocampus was performed in coronal sections (bregma −2.0 mm) and in the cerebellum on sagittal sections from three to six mice per group.

#### Statistical analysis

Data are presented as mean ± SEM; statistics were performed using the GraphPad Prism8 software (San Diego, CA). All data that passed the normality test (Shapiro-Wilk normality test) were analyzed using standard one-way analysis of variance (ANOVA). Kruskal-Wallis test followed by Dunn's post-hoc multiple comparison were used to analyze data that did not pass the normality test. Group comparisons were performed using two-way ANOVA with repeated measures when needed in behavioral and molecular studies, with treatment as the between-group factor and temporal or spatial variables (time in behavioral studies and different brain structure in molecular analysis) as the within factor, followed by Tukey (for one-way ANOVA) or Holm-Sidak (for two-way ANOVA) post-hoc multiple comparisons. Significance threshold was set at $p < 0.05$.

## DATA AVAILABILITY

The primary data for this study are available from the authors upon request.

## SUPPLEMENTAL INFORMATION

Supplemental information can be found online at https://doi.org/10.1016/j.omtn.2023.03.009.

## ACKNOWLEDGMENTS

This work was funded by the European Union's Horizon 2020 research and innovation program "Brain Involvement iN Dystrophinopathies" to F.M., C.V., and A.G., under grant agreement no. 847826. It was also supported by the Centre National de la Recherche Scientifique (CNRS, France), the Institut National de la Santé et de la Recherche Médicale (INSERM), the Université Paris-Saclay (France), Paris Ile-de-France Region, a project award from Association Monégasque contre les Myopathies (AMM, Monaco) to C.V. and a PhD fellowship from the Ministère de l'Enseignement Supérieur et de la Recherche (France) to A.S. We thank Dr. Katsuki Motoya and Prof. Sasaoka Toshikuni (Department of Comparative & Experimental Medicine/Brain Research Institute; Niigata University, Japan), and Dr. Jun Tanihata and Dr. Shin'ichi Takeda (National Center of Neurology and Psychiatry, Tokyo, Japan) for providing the *mdx52* mouse breeders. We thank Dr. Zarrouki for his advice. We are grateful to the Zootechnic platform of our institutes for mouse breeding, care, and to the genotyping platform.

## AUTHOR CONTRIBUTIONS

Conceptualization, C.V., F.M., and A.G.; methodology, A.S., C.V., and A.G.; investigation, A.S., S.B., O.l.C., O.V., M.D.C., T.T., and E.S.; writing – original draft, A.S., C.V., and A.G.; writing – review & editing, F.M., C.V., and A.G.; funding acquisition, F.M., C.V., L.G., and A.G.; supervision, C.V. and A.G.

## DECLARATION OF INTERESTS

T.T. and E.S. are employees of SQY Therapeutics, which produces tricyclo-DNA oligomers. L.G. is a co-founder of SQY Therapeutics.

## REFERENCES

1. Colombo, P., Nobile, M., Tesei, A., Civati, F., Gandossini, S., Mani, E., Molteni, M., Bresolin, N., and D'Angelo, G. (2017). Assessing mental health in boys with Duchenne muscular dystrophy: emotional, behavioural and neurodevelopmental profile in an Italian clinical sample. Eur. J. Paediatr. Neurol. *21*, 639–647. https://doi.org/10.1016/j.ejpn.2017.02.007.

2. Hinton, V.J., Cyrulnik, S.E., Fee, R.J., Batchelder, A., Kiefel, J.M., Goldstein, E.M., Kaufmann, P., and De Vivo, D.C. (2009). Association of autistic spectrum disorders with dystrophinopathies. Pediatr. Neurol. *41*, 339–346. https://doi.org/10.1016/j.pediatrneurol.2009.05.011.

3. Ricotti, V., Mandy, W.P.L., Scoto, M., Pane, M., Deconinck, N., Messina, S., Mercuri, E., Skuse, D.H., and Muntoni, F. (2016). Neurodevelopmental, emotional, and behavioural problems in Duchenne muscular dystrophy in relation to underlying dystrophin gene mutations. Dev. Med. Child Neurol. *58*, 77–84. https://doi.org/10.1111/dmcn.12922.

4. Knuesel, I., Zuellig, R.A., Schaub, M.C., and Fritschy, J.M. (2001). Alterations in dystrophin and utrophin expression parallel the reorganization of GABAergic synapses in a mouse model of temporal lobe epilepsy. Eur. J. Neurosci. *13*, 1113–1124. https://doi.org/10.1046/j.0953-816x.2001.01476.x.

5. Lidov, H.G., Selig, S., and Kunkel, L.M. (1995). Dp140: a novel 140 kDa CNS transcript from the dystrophin locus. Hum. Mol. Genet. *4*, 329–335. https://doi.org/10.1093/hmg/4.3.329.

6. Morris, G.E., Simmons, C., and Nguyen, T.M. (1995). Apo-dystrophins (Dp140 and Dp71) and dystrophin splicing isoforms in developing brain. Biochem. Biophys. Res. Commun. *215*, 361–367. https://doi.org/10.1006/bbrc.1995.2474.

7. Belmaati Cherkaoui, M., Vacca, O., Izabelle, C., Boulay, A.-C., Boulogne, C., Gillet, C., Barnier, J.-V., Rendon, A., Cohen-Salmon, M., and Vaillend, C. (2021). Dp71 contribution to the molecular scaffold anchoring aquaporine-4 channels in brain macroglial cells. Glia *69*, 954–970. https://doi.org/10.1002/glia.23941.

8. Desguerre, I., Christov, C., Mayer, M., Zeller, R., Becane, H.-M., Bastuji-Garin, S., Leturcq, F., Chiron, C., Chelly, J., and Gherardi, R.K. (2009). Clinical heterogeneity of duchenne muscular dystrophy (DMD): definition of sub-phenotypes and predictive criteria by long-term follow-up. PLoS One *4*, e4347. https://doi.org/10.1371/journal.pone.0004347.

9. Taylor, P.J., Betts, G.A., Maroulis, S., Gilissen, C., Pedersen, R.L., Mowat, D.R., Johnston, H.M., and Buckley, M.F. (2010). Dystrophin gene mutation location and the risk of cognitive impairment in Duchenne muscular dystrophy. PLoS One *5*, e8803. https://doi.org/10.1371/journal.pone.0008803.

10. Saoudi, A., Zarrouki, F., Sebrié, C., Izabelle, C., Goyenvalle, A., and Vaillend, C. (2021). Emotional behavior and brain anatomy of the mdx52 mouse model of Duchenne muscular dystrophy. Dis. Model. Mech. *14*, dmm049028. https://doi.org/10.1242/dmm.049028.

11. Vaillend, C., and Chaussenot, R. (2017). Relationships linking emotional, motor, cognitive and GABAergic dysfunctions in dystrophin-deficient mdx mice. Hum. Mol. Genet. *26*, 1041–1055. https://doi.org/10.1093/hmg/ddx013.

12. Vaillend, C., Rendon, A., Misslin, R., and Ungerer, A. (1995). Influence of dystrophin-gene mutation on mdx mouse behavior. I. Retention deficits at long delays in spontaneous alternation and bar-pressing tasks. Behav. Genet. *25*, 569–579. https://doi.org/10.1007/BF02327580.

13. Araki, E., Nakamura, K., Nakao, K., Kameya, S., Kobayashi, O., Nonaka, I., Kobayashi, T., and Katsuki, M. (1997). Targeted disruption of exon 52 in the mouse dystrophin gene induced muscle degeneration similar to that observed in Duchenne muscular dystrophy. Biochem. Biophys. Res. Commun. *238*, 492–497. https://doi.org/10.1006/bbrc.1997.7328.

14. Aartsma-Rus, A., Janson, A.a.M., Heemskerk, J.A., De Winter, C.L., Van Ommen, G.-J.B., and Van Deutekom, J.C.T. (2006). Therapeutic modulation of DMD splicing by blocking exonic splicing enhancer sites with antisense oligonucleotides. Ann. N. Y. Acad. Sci. *1082*, 74–76. https://doi.org/10.1196/annals.1348.058.

15. Dunckley, M.G., Manoharan, M., Villiet, P., Eperon, I.C., and Dickson, G. (1998). Modification of splicing in the dystrophin gene in cultured Mdx muscle cells by antisense oligoribonucleotides. Hum. Mol. Genet. *7*, 1083–1090. https://doi.org/10.1093/hmg/7.7.1083.

16. Mann, C.J., Honeyman, K., Cheng, A.J., Ly, T., Lloyd, F., Fletcher, S., Morgan, J.E., Partridge, T.A., and Wilton, S.D. (2001). Antisense-induced exon skipping and synthesis of dystrophin in the mdx mouse. Proc. Natl. Acad. Sci. USA *98*, 42–47. https://doi.org/10.1073/pnas.98.1.42.

17. Aoki, Y., Nakamura, A., Yokota, T., Saito, T., Okazawa, H., Nagata, T., and Takeda, S. (2010). In-frame dystrophin following exon 51-skipping improves muscle pathology and function in the exon 52-deficient mdx mouse. Mol. Ther. *18*, 1995–2005. https://doi.org/10.1038/mt.2010.186.

18. Aupy, P., Zarrouki, F., Sandro, Q., Gastaldi, C., Buclez, P.-O., Mamchaoui, K., Garcia, L., Vaillend, C., and Goyenvalle, A. (2020). Long-Term efficacy of AAV9-U7snRNA-mediated exon 51 skipping in mdx52 mice. Mol. Ther. Methods Clin. Dev. *17*, 1037–1047. https://doi.org/10.1016/j.omtm.2020.04.025.

19. Ferlini, A., Goyenvalle, A., and Muntoni, F. (2021). RNA-targeted drugs for neuromuscular diseases. Science *371*, 29–31. https://doi.org/10.1126/science.aba4515.

20. Goyenvalle, A., Griffith, G., Babbs, A., El Andaloussi, S., Ezzat, K., Avril, A., Dugovic, B., Chaussenot, R., Ferry, A., Voit, T., et al. (2015). Functional correction in mouse models of muscular dystrophy using exon-skipping tricyclo-DNA oligomers. Nat. Med. *21*, 270–275. https://doi.org/10.1038/nm.3765.

21. Relizani, K., Griffith, G., Echevarría, L., Zarrouki, F., Facchinetti, P., Vaillend, C., Leumann, C., Garcia, L., and Goyenvalle, A. (2017). Efficacy and safety profile of tricyclo-DNA antisense oligonucleotides in duchenne muscular dystrophy mouse model. Mol. Ther. Nucleic Acids *8*, 144–157. https://doi.org/10.1016/j.omtn.2017.06.013.

22. Relizani, K., Echevarría, L., Zarrouki, F., Gastaldi, C., Dambrune, C., Aupy, P., Haeberli, A., Komisarski, M., Tensorer, T., Larcher, T., et al. (2022). Palmitic acid conjugation enhances potency of tricyclo-DNA splice switching oligonucleotides. Nucleic Acids Res. *50*, 17–34. https://doi.org/10.1093/nar/gkab1199.

23. Robin, V., Griffith, G., Carter, J.-P.L., Leumann, C.J., Garcia, L., and Goyenvalle, A. (2017). Efficient SMN rescue following subcutaneous tricyclo-DNA antisense oligonucleotide treatment. Mol. Ther. Nucleic Acids *7*, 81–89. https://doi.org/10.1016/j.omtn.2017.02.009.

24. Zarrouki, F., Relizani, K., Bizot, F., Tensorer, T., Garcia, L., Vaillend, C., and Goyenvalle, A. (2022). Partial restoration of brain dystrophin and behavioral deficits by exon skipping in the muscular dystrophy X-linked (mdx) mouse. Ann. Neurol. *92*, 213–229. https://doi.org/10.1002/ana.26409.

25. Sekiguchi, M., Zushida, K., Yoshida, M., Maekawa, M., Kamichi, S., Yoshida, M., Sahara, Y., Yuasa, S., Takeda, S., and Wada, K. (2009). A deficit of brain dystrophin impairs specific amygdala GABAergic transmission and enhances defensive behaviour in mice. Brain *132*, 124–135. https://doi.org/10.1093/brain/awn253.

26. Goyenvalle, A., Vulin, A., Fougerousse, F., Leturcq, F., Kaplan, J.-C., Garcia, L., and Danos, O. (2004). Rescue of dystrophic muscle through U7 snRNA-mediated exon skipping. Science *306*, 1796–1799. https://doi.org/10.1126/science.1104297.

27. Aartsma-Rus, A., Straub, V., Hemmings, R., Haas, M., Schlosser-Weber, G., Stoyanova-Beninska, V., Mercuri, E., Muntoni, F., Sepodes, B., Vroom, E., and Balabanov, P. (2017). Development of exon skipping therapies for duchenne muscular dystrophy: a critical Review and a perspective on the outstanding issues. Nucleic Acid Therapeut. *27*, 251–259. https://doi.org/10.1089/nat.2017.0682.

28. Syed, Y.Y. (2016). Eteplirsen: first global approval. Drugs *76*, 1699–1704. https://doi.org/10.1007/s40265-016-0657-1.

29. Rigo, F., Chun, S.J., Norris, D.A., Hung, G., Lee, S., Matson, J., Fey, R.A., Gaus, H., Hua, Y., Grundy, J.S., et al. (2014). Pharmacology of a central nervous system delivered 2'-O-Methoxyethyl-Modified survival of motor neuron splicing oligonucleotide in mice and nonhuman primates. J. Pharmacol. Exp. Therapeut. *350*, 46–55. https://doi.org/10.1124/jpet.113.212407.

30. Hwang, K.-D., Kim, S.J., and Lee, Y.-S. (2022). Cerebellar circuits for classical fear conditioning. Front. Cell. Neurosci. *16*, 836948. https://doi.org/10.3389/fncel.2022.836948.

31. Hashimoto, Y., Kuniishi, H., Sakai, K., Fukushima, Y., Du, X., Yamashiro, K., Hori, K., Imamura, M., Hoshino, M., Yamada, M., et al. (2022). Brain Dp140 alters glutamatergic transmission and social behaviour in the mdx52 mouse model of Duchenne muscular dystrophy. Prog. Neurobiol. *216*, 102288. https://doi.org/10.1016/j.pneurobio.2022.102288.

32. García-Rodríguez, R., Hiller, M., Jiménez-Gracia, L., van der Pal, Z., Balog, J., Adamzek, K., Aartsma-Rus, A., and Spitali, P. (2020). Premature termination codons in the DMD gene cause reduced local mRNA synthesis. Proc. Natl. Acad. Sci. USA *117*, 16456–16464. https://doi.org/10.1073/pnas.1910456117.

33. Spitali, P., van den Bergen, J.C., Verhaart, I.E.C., Wokke, B., Janson, A.A.M., van den Eijnde, R., den Dunnen, J.T., Laros, J.F.J., Verschuuren, J.J.G.M., 't Hoen, P.A.C., and Aartsma-Rus, A. (2013). DMD transcript imbalance determines dystrophin levels. Faseb. J. *27*, 4909–4916. https://doi.org/10.1096/fj.13-232025.

34. Chesshyre, M., Ridout, D., Hashimoto, Y., Ookubo, Y., Torelli, S., Maresh, K., Ricotti, V., Abbott, L., Gupta, V.A., Main, M., et al. (2022). Investigating the role of dystrophin isoform deficiency in motor function in Duchenne muscular dystrophy. J. Cachexia Sarcopenia Muscle *13*, 1360–1372. https://doi.org/10.1002/jcsm.12914.

35. Beastrom, N., Lu, H., Macke, A., Canan, B.D., Johnson, E.K., Penton, C.M., Kaspar, B.K., Rodino-Klapac, L.R., Zhou, L., Janssen, P.M.L., and Montanaro, F. (2011). mdx($^5$cv) mice manifest more severe muscle dysfunction and diaphragm force deficits than do mdx Mice. Am. J. Pathol. *179*, 2464–2474. https://doi.org/10.1016/j.ajpath.2011.07.009.

36. Lindsay, A., Trewin, A.J., Sadler, K.J., Laird, C., Della Gatta, P.A., and Russell, A.P. (2021). Sensitivity to behavioral stress impacts disease pathogenesis in dystrophin-deficient mice. Faseb. J. *35*, e22034. https://doi.org/10.1096/fj.202101163RR.

37. Matsuzaka, Y., Tanihata, J., Ooshima, Y., Yamada, D., Sekiguchi, M., Miyatake, S., Aoki, Y., Terumitsu, M., Yashiro, R., Komaki, H., et al. (2020). The nSMase2/Smpd3 gene modulates the severity of muscular dystrophy and the emotional stress response in mdx mice. BMC Med. *18*, 343. https://doi.org/10.1186/s12916-020-01805-5.

38. Razzoli, M., Lindsay, A., Law, M.L., Chamberlain, C.M., Southern, W.M., Berg, M., Osborn, J., Engeland, W.C., Metzger, J.M., Ervasti, J.M., and Bartolomucci, A. (2020). Social stress is lethal in the mdx model of Duchenne muscular dystrophy. EBioMedicine *55*, 102700. https://doi.org/10.1016/j.ebiom.2020.102700.

39. Paxinos, G., and Franklin, K.B.J. (2001). The Mouse Brain in Stereotaxic Coordinates, Second Edition 2nd edition (Academic Press).

40. Goyenvalle, A., Babbs, A., Wright, J., Wilkins, V., Powell, D., Garcia, L., and Davies, K.E. (2012). Rescue of severely affected dystrophin/utrophin-deficient mice through scAAV-U7snRNA-mediated exon skipping. Hum. Mol. Genet. *21*, 2559–2571. https://doi.org/10.1093/hmg/dds082.

41. Paylor, R., Zhao, Y., Libbey, M., Westphal, H., and Crawley, J.N. (2001). Learning impairments and motor dysfunctions in adult Lhx5-deficient mice displaying hippocampal disorganization. Physiol. Behav. *73*, 781–792. https://doi.org/10.1016/s0031-9384(01)00515-7.

42. Chaussenot, R., Edeline, J.-M., Le Bec, B., El Massioui, N., Laroche, S., and Vaillend, C. (2015). Cognitive dysfunction in the dystrophin-deficient mouse model of Duchenne muscular dystrophy: a reappraisal from sensory to executive processes. Neurobiol. Learn. Mem. *124*, 111–122. https://doi.org/10.1016/j.nlm.2015.07.006.

43. Echevarría, L., Aupy, P., Relizani, K., Bestetti, T., Griffith, G., Blandel, F., Komisarski, M., Haeberli, A., Svinartchouk, F., Garcia, L., and Goyenvalle, A. (2019). Evaluating the impact of variable phosphorothioate content in tricyclo-DNA antisense oligonucleotides in a duchenne muscular dystrophy mouse model. Nucleic Acid Therapeut. *29*, 148–160. https://doi.org/10.1089/nat.2018.0773.